Determining the modulus of soils with the pressuremeter test

CAMBRIDGE INSITU LTD

Contents

Determining the modulus of soils with the pressuremeter test

Terms:

G_P	Pressuremeter shear modulus
G_S	Secant shear modulus
G_T	Tangential shear modulus
G_y	Secant shear modulus at the maximum elastic shear strain
G_{HH}, G_{VH}	Shear moduli for transversely isotropic material
E_H, E_V	Young's modulus in the horizontal and vertical direction
ν_{HH}, ν_{HV}	Poisson's ratios for transversely isotropic material
n	Ratio of horizontal to vertical Young's modulus E_H/E_V
N	Exponent (Whittle & Liu, 2013)
K_O	Ratio of horizontal to vertical effective insitu stress
τ	Shear stress
p_C	Pressure measured at the cavity wall
ε_c	Circumferential strain measured at the borehole wall
γ	Shear strain
γ_c	Shear strain measured at the borehole wall
γ_a	Invariant shear strain (axial strain in a triaxial test)
η	Radial stress intercept
β	Elastic exponent
α	Shear stress intercept
σ'_{av}	Mean effective stress
σ_{ho} σ'_{ho}	Total and effective insitu lateral stress
σ_{vo} σ'_{vo}	Total and effective insitu vertical stress

Background

Figure 1 **Field curve –pre-bored test in silty sand**

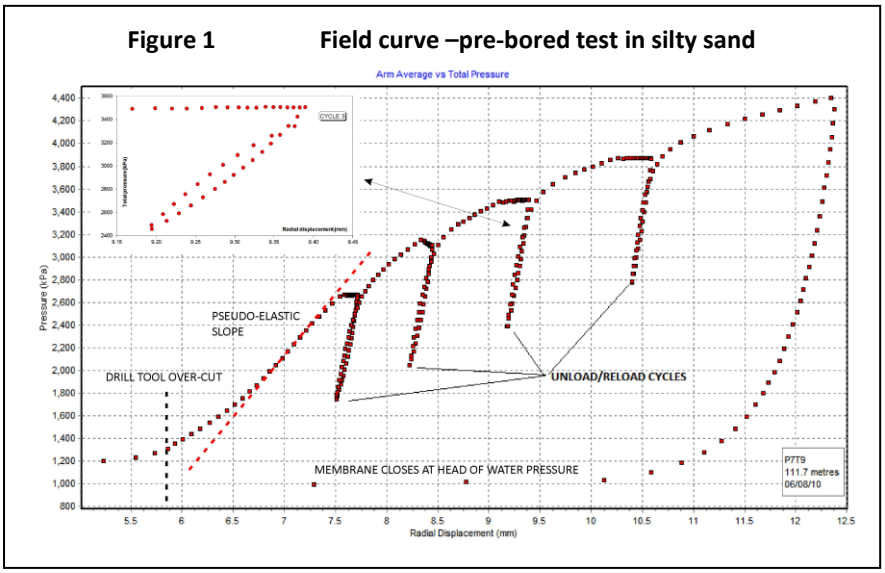

The interpretation of the pressuremeter test must take account of the disturbance caused by the method used to place the probe in the ground. The least disruptive of the methods is self boring where disturbance is usually small enough to not cause the material to fail and is therefore recoverable. The alternatives to self bored devices are pre-bored probes or pushed instruments such as the Cone Pressuremeter (CPM). In soils the disturbance caused by pre-boring is seldom recoverable and for pushing is never recoverable because during the push the material will have been taken to a limit condition. The material is likely to be in a complex stress state

prior to the expansion phase of the test commencing. In seems therefore that using the loading curve as a source of stiffness data is questionable due to the unknowable contribution of disturbance effects.

However for any insertion process it is possible to erase the previous stress history by extending the zone of failed material and putting every element of soil within the zone into a uniform plastic condition. At a remote radius from the pressuremeter there is a boundary where the material is on the point of yielding. If the direction of loading is reversed, the response seen at the pressuremeter will be that of the remote boundary being unloaded elastically, and eventually plastically if the process is taken far enough. In fig 1 the unload/reload cycles rely on this principle to allow the true elastic properties of the ground to be discovered. It is evident that although each cycle is taken at a different expansion the response is highly repeatable. This test was pre-bored, so the cavity was completely unloaded prior to the pressuremeter test commencing. The consequences of this are obvious when the slope of the initial loading is compared to the unload/reload cycles.

The displacement changes within the cycles are small and do not cause the material to yield in extension. The third cycle in fig 1 is shown as an inset, and it can be seen that it has a hysteretic characteristic. This is due to the influence of strain level on the current modulus. Bolton & Whittle (1999) shows that for shear strains above 10^{-4} this non-linear response is adequately described by a power curve, permitting the stiffness degradation curve to be defined (fig 2).

Figure 2 **Shear modulus degradation curves**

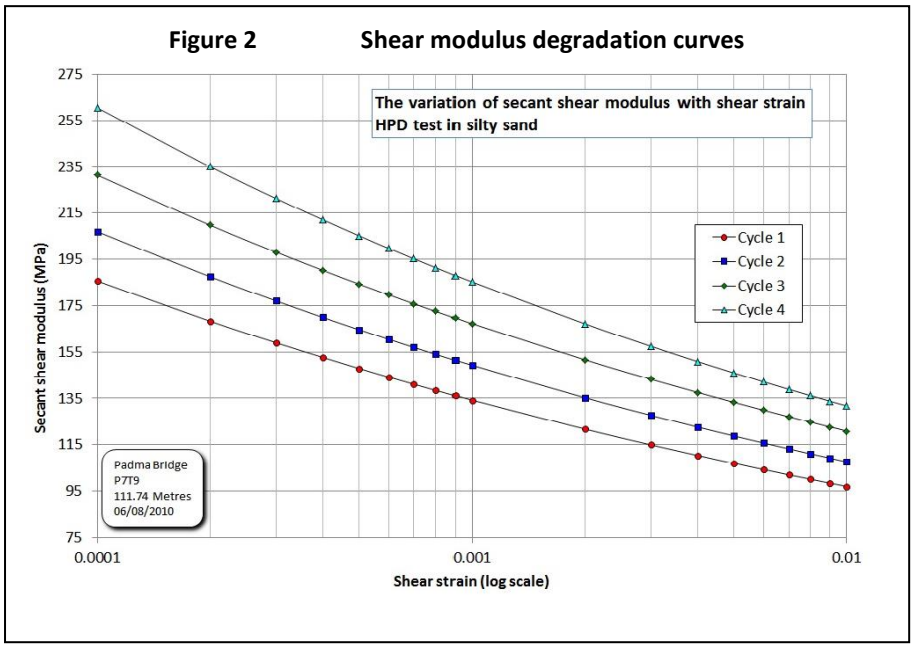

In this material the shape of each cycle (the strain dependency) is almost identical, but successive cycles plot a higher stiffness, because of changing stress level. If the material was low permeability clay giving an undrained loading then the mean effective stress σ'_{av} following yield is constant, and all cycles would plot the same stiffness/strain curve. In this material, silty sand, the loading is drained and σ'_{av} is increasing throughout, giving the response seen in fig 2. Part of the data reduction procedure is to adjust these trends to a reference stress level such as the effective insitu lateral stress, σ'_{ho}. This requires the σ'_{av} for each cycle to be calculated. Hence although in principle stiffness is obtainable from all pressuremeter tests, no matter how disturbed the insertion process, it remains necessary to determine additional engineering parameters in order fully to reconcile the stiffness data.

Pressuremeter derived stiffness is also affected by cross anisotropy. The pressuremeter used conventionally gives shear modulus parameters of type G_{HH}, where the first suffix

shows the direction of loading and the second suffix the direction of particle movement. Many design calculations that require a value for shear modulus mean in practice the independent shear modulus $G_{VH.}$ Translating between pressuremeter values and alternative expressions for modulus is complex but worth pursuing because of the high quality and speed of the pressuremeter measure.

Unloading and reloading are a feature of certain triaxial procedures and pile loading experiments. In the context of pressuremeters the first account of the theory behind the procedure is given by Hughes'82. Cycles are a prominent feature of the Wroth Rankine lecture (Wroth, '84). Bellotti et al ('89) give a clear explanation and methodology for manipulating the stress dependency of tests in sand. A number of authors in the 1990's, especially Muir Wood (1990) and Jardine (1992) explore the non-linear strain dependency characteristic of the cycles. Bolton & Whittle ('99) propose the simple procedure described below, using a power function to discover the non-linear strain components. Whittle ('99) shows how the power function approach relates to the solution of Palmer ('72) for the current mobilised shear stress at any part of the undrained pressuremeter curve.

This methodology is extensively used in the United Kingdom, perhaps because of the greater use of high resolution pressuremeters with local measurement – it is almost impossible to make plausible unload/reload cycles with simpler equipment such as the Ménard pressuremeter, where the resolution of expansion change is too poor to see an elastic strain alteration.

Linear elastic interpretation

If the material was linear elastic then the slope of a line bisecting the apices of a cycle could be used to derive the shear modulus. Figure 3 shows a typical example of one such cycle.

The equation used is: $G = \Delta p_c / 2\Delta\varepsilon_c$ Equ.[1]

Implicit in this equation is the assumption that Δp_c is equivalent to $\Delta\tau_c$, that is to say the material has linear elastic characteristics. Note that the cavity strain calculation uses the measured radial displacement at the centre of the cycle as a strain origin, so every cycle has a different origin.

Fig 3 Expanded view of an unload/reload cycle

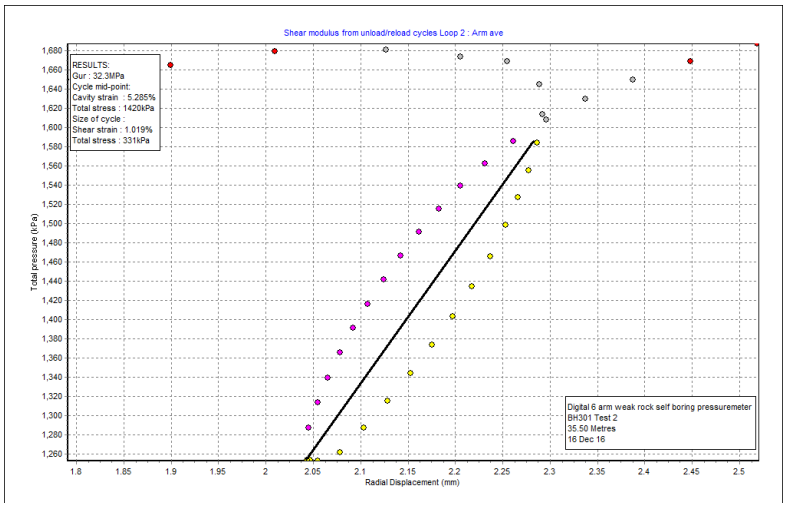

Ideally the loop should be conducted with as little interruption to the loading as possible but it is sometimes necessary to hold the pressure in the probe for a short time (maybe as little as a minute) prior to starting to unload.

The pressuremeter test is a shearing process. The modulus measured is a function of shear modulus G and is independent of Poisson's ratio, although this is not always obvious from the way in which modulus data are sometimes presented.

The linear-elastic approach is likely to be valid only for tests in rock.

Non-linear stiffness/strain response

It is now widely acknowledged that below the strain necessary to cause the material to yield, the stiffness/strain relationship is not linear. The unload/reload cycle can be made to give a comprehensive description of this non-linear relationship by looking at smaller steps of pressure/strain other than the points at the extreme ends of the cycle.

Fig 4 Annotated unload/reload cycle

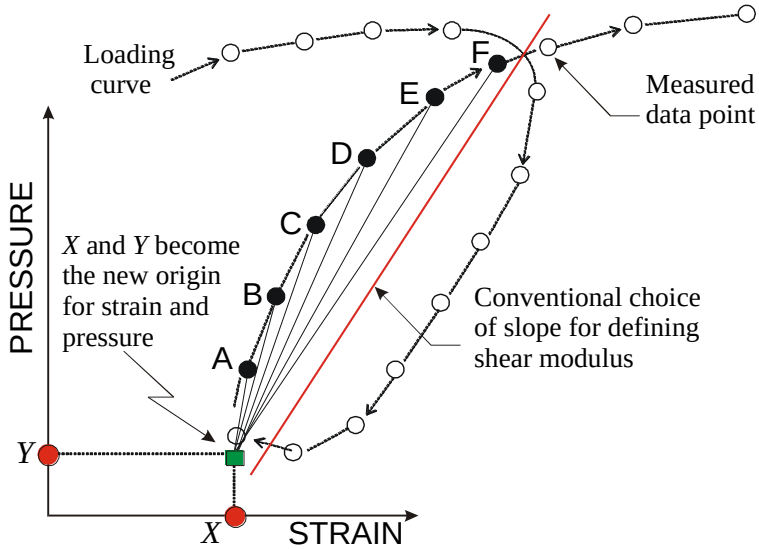

For reasons explained in Whittle et al (1992) it is preferable to examine one half of the rebound cycle only, that which follows the reversal of stress in a loop. The lowest recorded value of stress and strain then becomes the origin for subsequent data points until the original loading path is re-joined.

In Fig 4, once a new origin is defined, every subsequent data point on the reloading part of the loop (A, B, C etc.) can be used to give a value for secant shear modulus. This value can then be plotted against the associated strain increment as measured from the new strain origin.

It follows that it is not necessary to take cycles of small strain amplitude in order to obtain small strain stiffness parameters. Indeed it is better to make the cycles as large as possible (subject to the condition that the material is not allowed to fail in extension) in order to obtain parameters for as wide a strain range as possible.

Using the local origin for each cycle the reloading data are plotted on log log axes of radial stress versus shear strain at the cavity wall, and the intercept and gradient of the best fit straight line is identified (fig 5). The gradient expresses the non-linearity of the response, so 1 would be linear elastic. In the example the gradient is 0.629.

If the expansion is undrained then Bolton & Whittle (1999) show how the intercept and gradient allow the equivalent trend in shear stress: shear strain space to be derived. The quickest proof is obtained by using the raw trend as input for the Palmer (1972) solution for undrained cavity expansion. For a test in drained material the same solution can be used assuming that whilst the material is deforming elastically *no volumetric strains* result.

In fig 5 the correspondence to a straight line is excellent, and a correlation co-efficient better than 0.98 is typical.

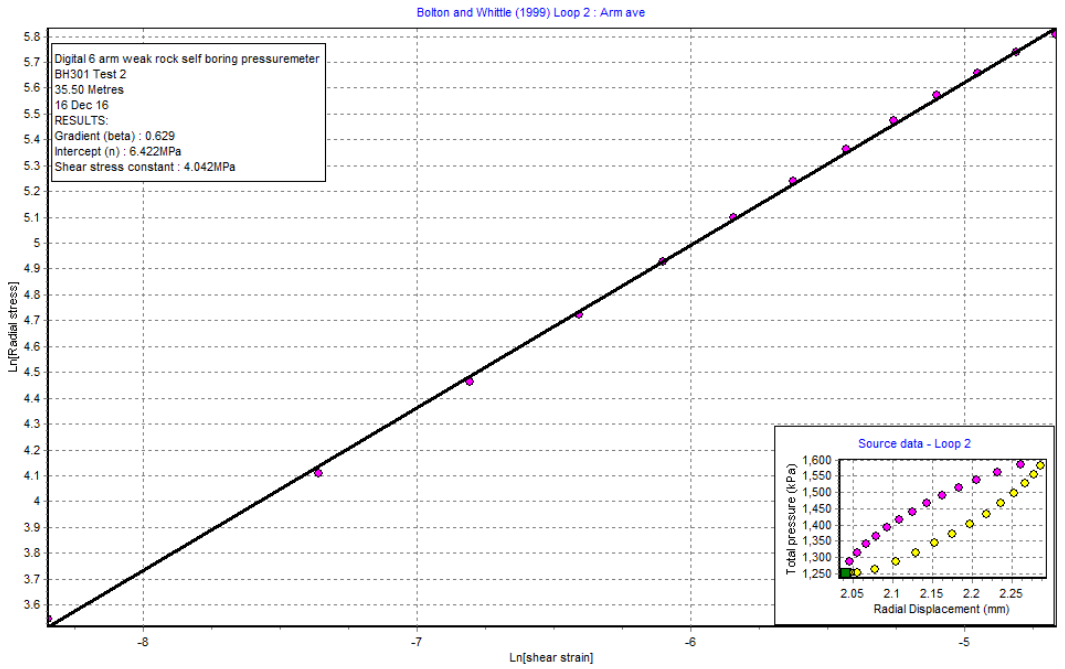

Fig 5 The non linear elastic response

From pressuremeter modulus to secant and tangential modulus

As shown in fig 5 the variation of stiffness with strain seen in a pressuremeter rebound cycle can be expressed as a power law. While the soil is responding elastically, pressure measured at the borehole wall is given by

$$p_c = \eta\gamma^{\beta} \qquad \text{Equ.[2]}$$

noting that γ is plane shear strain, approximately twice the cavity strain.

For clays, Palmer (1972) shows that the current shear stress τ_c is given by

$$\tau_c = dp/d[\ln(\gamma)] \qquad \text{Equ.[3]}$$

Substituting for dp using the right hand side of [2] allows the differential equation to be solved giving

$$\tau_c = \eta\beta\gamma^{\beta} \qquad \text{Equ.[4]}$$

$\eta\beta$ is the shear stress constant and is usually called α, a term defined by the Bolton & Whittle analysis. Shear modulus is shear stress divided by shear strain so secant shear modulus G_s is given by :

$$G_s = \alpha\gamma_c^{\beta-1} \qquad \text{Equ.[5]}$$

This gives a means of determining the secant shear modulus at any elastic shear strain, although an arbitrary cut-off strain must be assumed below which the modulus will be constant and a maximum – this strain is below the resolution of the current generation of

pressuremeters. It is our practice to quote between 10^{-4} and 10^{-2} plane shear strain (0.01% to 1%).

Note: When comparing triaxial results with pressuremeter results, invariant shear strain γ_a is $\gamma_a = \gamma_c / \sqrt{3}$

Tangential shear modulus G_t is given by (Muir Wood, 1990) $G_t = G_s + \varepsilon_c[dG_s/d\varepsilon_c]$ Equ.[7]

Hence from the power law $G_t = \alpha\beta\gamma_c^{\beta-1}$ Equ.[8]

For the purpose of finding the single value of secant shear stiffness governing the pressuremeter response seen in the measured loading curve, G_y is required. This is the secant modulus at the maximum elastic shear strain. It is too conservative a value for design purposes.

Stress level

For modulus parameters derived from undrained expansion tests the mean effective stress remains unchanged throughout the expansion and all stiffness:strain data will plot the same trend. Conversely, failure to plot the same trend implies changes in the mean effective stress (fig 2).

Whittle & Liu (2013) give a method for both stress and strain adjustment. It is based on Bellotti et al (1989) and can be applied to tests that contain at least four unload/reload cycles.

Their solution can be written as: $G = A\sigma^N$ Equ.[9]

A and N are both semi-log equations. For most purposes this level of complexity is not required and a simpler approach can be adopted.

1) Start by carrying out the non-linear analysis described above and discover α and β. Use these to find, for each cycle, G_s at an intermediate value of shear strain, such as 0.1%.
2) Calculate the mean effective stress σ'_{av} at the commencement of each loop. The effective radial stress p' is measured by the pressuremeter and the calculation is

$$\sigma'_{av} = p'/(1+\sin\phi) \quad \text{Equ.[10]}$$

where ϕ is the peak angle of internal friction

3) Plot modulus against effective stress (fig 6).

The example in fig 6 shows two tests in sand treated in this way. Each test gives a set of points that follow a power law trend. The exponent of the power law is describing the stress dependency at this level of shear strain. At this strain, typical values for the exponent are in the range 0.3 to 0.4. The correlation coefficient for each trend is better than 0.99.

Fig 6 Finding the stress dependency exponent

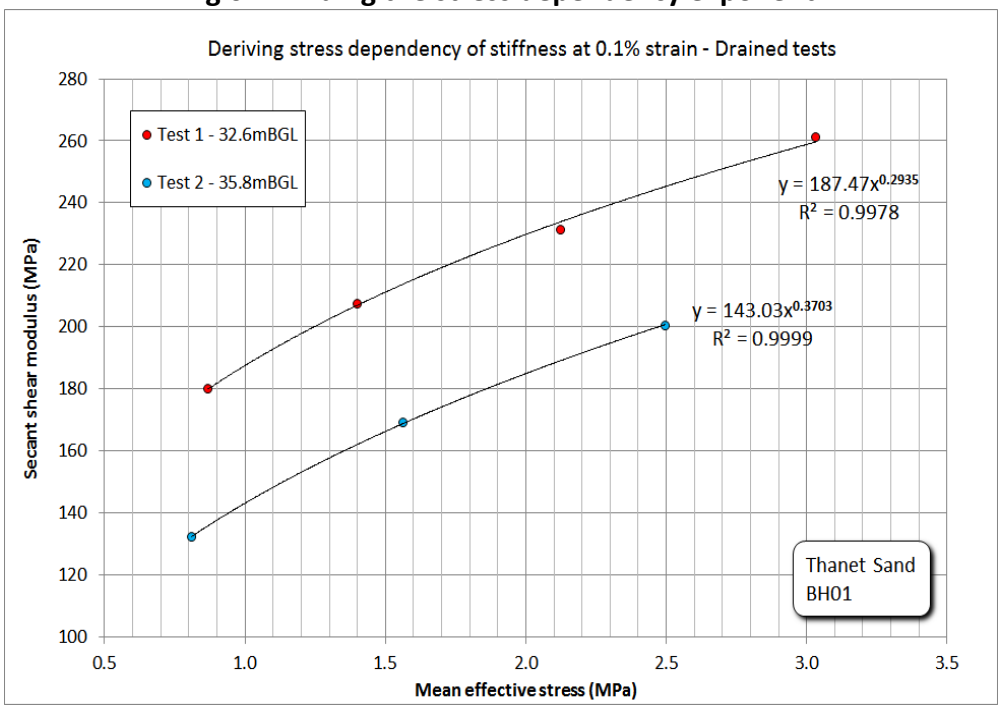

Given the stress dependency exponent n, , for each cycle a stress adjusted version of α is found, α*:

$$\alpha* = \alpha(\sigma'_{ref}/\sigma'_{av})^n \qquad \text{Equ.[11]}$$

[11] is based on the relationship suggested by Janbu ('63) and forms the basis of the

Fig 7 – Raw secant shear modulus

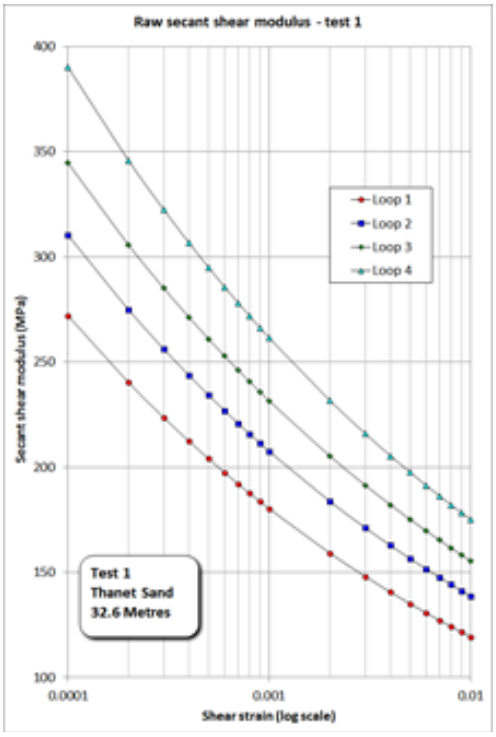

Fig 8 – Adjusted secant shear modulus

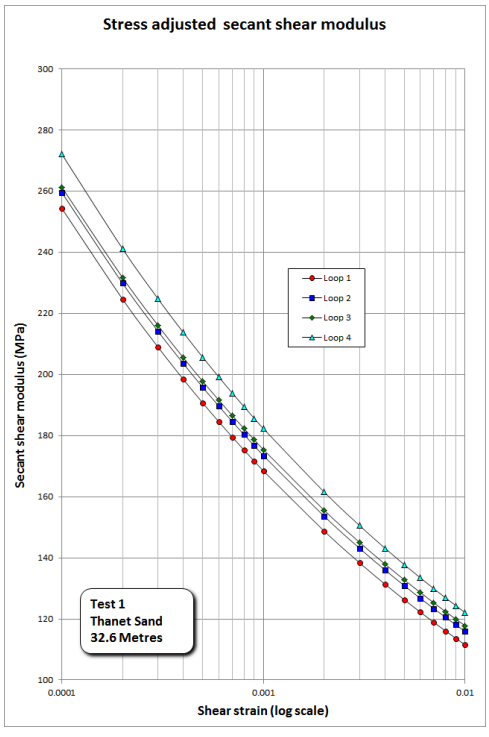

approach to stress dependency used in Bellotti et al (1989). The reference stress is typically σ'_{vo} or σ'_{ho}. For applications where a vertical deformation modulus is required it seems sensible to use σ'_{vo}. α^* is used in place of α in [5] to derive the stress adjusted modulus. Figs 7 and 8 give a 'before' and 'after' example of the method being applied.

Cross hole anisotropy

The pressuremeter test gives values for G_{HH}, the shearing stiffness in the horizontal plane. This is directly applicable to the analysis of radial consolidation or cylindrical cavity expansion due to pile insertion. G_{VH} is applicable all shearing which has an element of deformation in the vertical plane, such as under a footing or round an axially loaded pile.

To convert from G_{HH} to G_{VH} some relationship between the two must be assumed. Wroth et al (1979) suggest that anisotropy arises from two causes:

- Structural anisotropy due to the deposition of soil on well defined planes
- Stress induced anisotropy, due to the differences in normal stress acting in different directions.

The second cause implies the stiffness in any direction will be a function of the effective insitu stress in that direction, ie a function of K_O.

It can be shown	$G_{HH} = E_H/[2(1+\nu_{HH})]$	Equ.[12]
For undrained expansion	$\nu_{HH} = 1-m/2$	Equ.[13]
and	$m = E_H/E_V = K_O$	Equ.[14]
From this it follows	$E_H = (4-m)G_{HH}$	Equ.[15]
and	$E_V = (4-m)G_{HH}/m$	Equ.[16]

This is as far as argument from first principles can go, because of the additional contribution of the manner in which the material is deposited. K_O is likely to lie between 0.5 and 2, so from [14] E_H/G_{HH} lies between 2 and 3.5. From [16] E_V/G_{HH} lies between 1 and 1.75.

It is likely that G_{VH} will be linked to E_V by Poisson's ratio in a relationship of the form of [16]. Plausible values of E_V/G_{VH} would seem to be 2.4 to 3. Hence in a material with K_O of 2, G_{VH} could be as low as $G_{HH}/3$. Simpson et al (1996) come to the same conclusion, but find in practice heavily over-consolidated London clay gives relationships of the order of $G_{VH} \cong 0.65G_{HH}$. The influence of the strain range is not separately considered in these studies.

Lee & Rowe (1989) give details of the anisotropy characteristics of many clays varying from lightly overconsolidated to heavily overconsolidated. The general conclusion is E_V/G_{VH} lies between 4 and 5, rather more than the isotropic relationship of 3. However their paper was concerned with the impact of anisotropic stiffness properties on surface settlement. Deriving G_{VH} from E_V is therefore unsatisfactory, because although G_{VH} is insensitive to the direction of loading, E_V is not.

Shear modulus from other parts of the pressuremeter curve.

The initial part of the loading will give a value for secant shear modulus, usually referred to as G_i. Provided the insertion disturbance is low this will be a plausible value but affected by the same considerations of stress level and strain range as other parts of the curve.

The first part of the unloading can in principle give a similar parameter but by the time the pressuremeter unloads the creep strains due to consolidation and rate effects will be large, so there will be a tendency for the initial unloading to be too stiff. However provided some allowance is made for this then reasonable estimates of the shear modulus will be obtained.

Curve fitting analyses imply a value for the secant shear modulus at yield. Although this is not likely to be the best way of deriving shear modulus data it is important justification for using such analyses that they can predict this independently measurable stiffness.

Young's Modulus

All modulus parameters derived from the pressuremeter test are shear modulus G_{HH}. They can be converted to Young's modulus E_{HH} using [12], above.

A non-linear version of [12] is $E = 2\alpha(1+ v)(\sqrt{3}\gamma_a)^{\beta-1}$ Equ.[17]

This incorporates the power law parameters. γ_a is invariant or axial shear strain, so multiplying it by √3 (see the note above) has the effect of converting it to plane shear strain. This allows α and β parameters obtained in shear stress/plane shear strain space to be applied.

Non-linear modulus in terms of shear stress

For some applications it is convenient to derive stiffness values as a proportion of the mobilized strength. If the shear strength c_u is known, and *x* represents the proportion of strength used, then the shear strain γ_x for this proportion is given as follows:

Where $0 < x \leq 1$ $\gamma_x = [xc_u/\alpha]^{(1/\beta)}$ Equ. [18]

For example it is common to require G_{50}, the shear modulus when half of the available strength is mobilised. It is straightforward to apply the preceding non-linear stiffness expressions to derive the relevant modulus:

Generally, shear modulus at strength fraction z: $G_z= \alpha[zc_u/\alpha]^{(1-\beta)/\beta}$ Equ. [19]

Specifically, for G_{50}: $G_{50}= \alpha[c_u/2\alpha]^{(1-\beta)/\beta}$ Equ. [20]

Possible method for estimating G_{max} and the threshold elastic shear strain.

Oztoprak and Bolton (2013) present a methodology for deriving stiffness/strain curves from a limited set of information for a particular material. One of the relationships they find useful is that due to Fahey & Carter (1993) where the ratio G/G_{max} is connected to a hyperbolic function using fractions of the shear stress to failure, as follows:

$$G/G_{max}= 1- f(\tau/\tau_f)^g \quad \text{Equ. [21]}$$

The f and g terms allow the curvature of the basic hyperbolic function to be manipulated. f will take a value close to but not greater than 1, say 0.9. g has more effect on the curvature and reported values applied to real soils lie in the range 0.25 to 0.35.The ratio τ/τ_f is analogous to z used in [19] so it is possible to write the following:

$$G_{max}= G_z /[1- f(z)^g] \quad \text{Equ. [22]}$$

Figure 9 is the result of applying [22] to a single cycle in London Clay. If the formulation of [21] was correct then all proportions of stress would give the same answer. Clearly they do

not but the major discrepancies occur at the limits of the trend. Within the proportion range 0.1 to 0.6 there is reasonable agreement. Presumably the errors are due to the mismatch between a hyperbolic decay curve being mapped onto a power law trend.

Published uses of [21] seem to be referred to tests in sand. There is no reason in principle why this approach should not be applied to a fine grained material. In fig 9, *f* has been chosen to give an equal error at the extremes of the stress ratio τ/τ_{ult} and in this example τ_{ult} is the undrained shear strength c_u. It seems reasonable to expect non-linearity to be greater in clays than sands, and so 0.2 has been used for *g*. Common sense suggests that G_{max} will start to decay at strains somewhere in the range 10^{-5} to 10^{-4} and this allows unrealistic values of *g* to be identified. A *g* of 0.35, for example, would make the threshold elastic shear strain 10^{-4}.

Fig 9 Inferring the maximum shear modulus

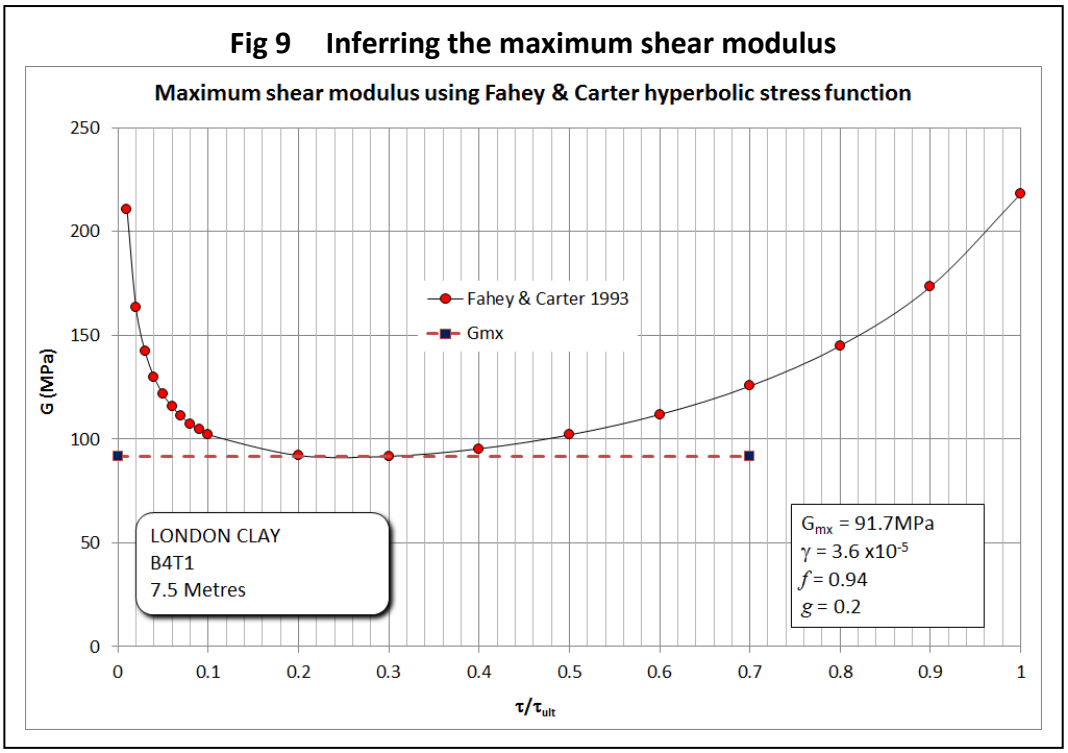

References

BELLOTTI, R., GHIONNA, V., JAMIOLKOWSKI, M., ROBERTSON, P. and PETERSON, R. (1989).
Interpretation of moduli from self-boring pressuremeter tests in sand. *Géotechnique* Vol.**39**, no.2, pp.269-292.

BOLTON M.D. and WHITTLE R.W. (1999)
A non-linear elastic/perfectly plastic analysis for plane strain undrained expansion tests. *Géotechnique* Vol. **49**, No.1, pp 133-141.

FAHEY, M. (1992)
Shear modulus of cohesionless soil: variation with stress and strain level. Canadian Geotechnical Journal. Vol. 29, No. 1, pp. 157-161.

FAHEY, M. AND CARTER, J.P. (1993)
A finite element study of the pressuremeter test in sand using a nonlinear elastic plastic model. Canadian Geotechnical Journal, Vol. 30, No. 2, pp. 348-362.

HUGHES, J.M.O. (1982)
Interpretation of pressuremeter tests for the determination of elastic shear modulus. *Proc.Engng Fdn Conf. Updating subsurface sampling of soils and rocks and their in-situ testing, Santa Barbara,* pp 279-289.

JANBU, N. (1963)
Soil compressibility as determined by oedometer and triaxial tests. *Proc. 3rd Eur. Conf. Soil Mech*., Wiesbaden 2, pp 19-24.

JARDINE, R.J. (1992)
Nonlinear stiffness parameters from undrained pressuremeter tests. *Can. Geotech*. **29**, pp 436-447

LEE, K.M. AND ROWE, R.K. (1989)
Deformations caused by surface loading and tunnelling: the role of elastic anisotropy. *Géotechnique* **39***,* No. 1, pp 125-140.

MUIR WOOD, D. (1990)
Strain dependent soil moduli and pressuremeter tests. *Géotechnique*, **40**, pp 509-512.

OZTOPRAK, S. & BOLTON, M. D. (2013)
Stiffness of sands through a laboratory test database *Géotechnique* **63**, No. 1, pp 54–70

SIMPSON, B., ATKINSON, J.H. AND JOVICIC,V. (1996)
The influence of anisotropy on calculations of ground settlements above tunnels. Proc. Int. Symp. Geotechnical aspects of Underground Construction in Soft Ground, City University, London, April.

WHITTLE R.W (1999)
Using non-linear elasticity to obtain the engineering properties of clay. *Ground Engineering*, May, vol. 32, no.5, pp 30-34.

WHITTLE R.W and LIU LIAN (2013)
A method for describing the stress and strain dependency of stiffness in sand. Proc. ISP6, Paris, 2013

WROTH, C.P. (1984)
The Interpretation of In Situ Soil Tests. Twenty Fourth Rankine Lecture, *Géotechnique* **34**, No. 4, pp 449-489

WROTH C.P., RANDOLPH M.F., HOULSBY G.T. AND FAHEY M. (1979)
A review of the engineering properties of soils with particular reference to the shear modulus. Cambridge University Engineering Department, Soils TR75.